RSC Advances

PAPER

View Article Online
View Journal | View Issue

Cite this: *RSC Adv.*, 2022, **12**, 12463

Grafting of thermotropic fluorinated mesogens on polysiloxane to improve the processability of linear low-density polyethylene†

Wenqing Wu, *[a] Pan Li,*[b] Xiaohang Wang[c] and Baoyan Zhang[d]

In this study, a series of polysiloxane grafted with thermotropic fluorinated mesogens (TSCPFLCP) is designed and synthesized. The TSCPFLCP exhibits a typical smectic liquid crystal phase, and shows a high thermal decomposition temperature at 335.6 °C. After blending with LLDPE, the balance melt torque of LLDPE/TSCPFLCP is decreased by 42% at 0.5 wt% TSCPFLCP, and the corresponding power law index is increased to 0.45. The flowing activation energy of the optimized LLDPE/TSCPFLCP blend is lower than that of pure LLDPE at the same shear rate, indicating that TSCPFLCP reduced the sensitivity of the apparent melt viscosity of LLDPE to both shear rate and temperature. This contributes to the broadening of the LLDPE processing window. On the other hand, TSCPFLCP is also found beneficial in ameliorating melt fracture during LLDPE extrusion. Furthermore, the mechanical properties of LLDPE/TSCPFLCP blends, such as tensile strength, elastic modulus and elongation at break, are also enhanced significantly at 0.5 wt% TSCPFLCP. Altogether, TSCPFLCP has been proven an effective processing aid to improve the processability and toughness of LLDPE.

Received 6th March 2022
Accepted 19th April 2022

DOI: 10.1039/d2ra01482c

rsc.li/rsc-advances

1. Introduction

To improve the processability of thermoplastic composites,[1,2] processing aids such as linear polydimethylsiloxane (PDMS) are frequently used in the production process due to their lubrication effect for plastics.[3,4] For instance, a minuscule amount of polysiloxane bearing long-chain alkyl side groups can significantly increase the melt flow rate to facilitate the processing process.[5] However, PDMS is a typical liquid polymer and cannot be conveniently handled in industrial production. As an alternative processing aid, thermotropic liquid crystalline polymer (TLCP) also exhibits excellent lubricating properties for thermoplastic polymer melts.[6–9] In the melting process, TLCPs in the liquid crystal phase are easily oriented and arranged along the flow direction under the action of shear force or tension, therefore improving the processability of thermoplastic composites.[10–14]

Nevertheless, the main drawback of most main chain TLCPs is the high melting temperature, and it greatly confines their use to engineering plastics which are tolerant of higher processing temperature.[15] In this regard, only few main chain TLCPs meet the requirement of low processing temperature system, such as polyolefin based thermoplastic composites.[16] Therefore, reducing the melting point of TLCPs is highly desirable to broaden their application.[17] On the other hand, ameliorating the melt fracture and reducing the extruder head pressure are also crucial to improve the polyolefins production efficiency. These improvements can be potentially achieved by integrating fluorinated compounds on TLCPs due to their excellent lubricating properties for processing thermoplastic materials.[18,19] To address these practical issues, we assume that a polysiloxane grafted by thermotropic fluorinated mesogenic unit (TSCPFLCP) is a new kind of powdered processing aid with low and tunable melting temperature. This is because TSCPFLCP comprises both the flexible PDMS segment as main chain and thermotropic mesogens on polymer side chain. Such a featured polymeric structure has been demonstrated to adjust the melting temperature between 15 ∼ 200 °C,[20] and the isotropic temperature between 84 ∼ 300 °C.[21,22] Meanwhile, the introduction of polar fluorine group is expected to significantly reduce the melt fracture during the processing of polyolefin.

Compared with PDMS and main chain TLCPs, TSCPFLCPs show potential advantages in industrial production, however, no related work has been reported to the author's knowledge. In the current work, a series of TSCPFLCPs with low melting temperature were successfully synthesized to blend with linear low-density polyethylene (LLDPE). The influence of TSCPFLCP loading on the processing and tensile properties of composite

[a]*School of Materials Science and Engineering, Northeastern University, Shenyang 110819, China. E-mail: wwq714wwq714@126.com*
[b]*School of Chemistry and Chemical Engineering, Hefei Normal University, Hefei 230601, China. E-mail: panli_hfnu@126.com*
[c]*China Chemical Technology Research Institute, Beijing 100029, China*
[d]*Center for Molecular Science and Engineering, Northeastern University, Shenyang 110819, China*

† Electronic supplementary information (ESI) available. See https://doi.org/10.1039/d2ra01482c

materials were investigated. In addition, the modification mechanism of LLDPE by TSCPFLCP under different processing temperatures, rotating speeds and shear rates was also studied to provide guidance for industrial processing. Overall, this study provides a feasible scheme for the synthesis of well-structured liquid crystal polymers to meet the special needs of plastic processing.

2. Experiment

2.1 Materials

(Trans, trans)-4-(3,4-difluorophenyl)-4′-vinyl-1,1′ bi(cyclohexane) (M_1) (T_m: 50.6 °C,T_i: 109.4 °C) and 1-but-3-enyl-4-(4-propylcyclohexyl)cyclohexane (M_2) (T_m: 74.8 °C, T_i: 79.2 °C) were purchased from Bayi Space LCD Technology (Beijing, China) Co., Ltd. Poly(methylhydrogeno)siloxane (PMHS, M_n = 582, M_w = 595, PDI = 1.02) were purchased from Aladdin Chemical Reagent Co., Ltd (Shanghai, China). Linear low-density polyethylene (LLDPE, DFDA 7042, MFI = 2.0 g/10 min, M_n = 30 400, M_w = 122 200, PDI = 4.02) was produced by Sinopec Guangzhou Co., Ltd (Guangzhou, China). Toluene, ethanol, tetrahydrofuran (THF) and methanol were purchased from Shenyang Chemical Co., Ltd (Shenyang, China).

2.2 Instruments

Fourier transform infrared spectra (FT-IR) were measured on PerkinElmer instruments Spectrum One Spectrometer (PerkinElmer, Foster City, CA, USA) after compressing samples into KBr pellets. ^{1}H-NMR was tested by a Varian WH-90PFT NMR Spectrometer (Varian Associates, Palo Alto, CA) with $CDCl_3$ and tetramethylsilane (TMS) as an internal standard. The thermal properties and curing studies were carried out with a NETZSCH Instruments DSC 204 (Netzsch, Wittelbacherstrasse, Germany) at heating and cooling rate of 10 °C min^{-1} under nitrogen atmosphere. The texture of monomers and cured products were observed with a polarized optical microscope (POM) (Leica, Wetzlar, Germany) equipped with a Linkam THMSE-600 (Linkam, Surrey, UK) hot stage connected to a TP-92 temperature control unit. Wide-angle X-ray diffraction measurements were performed on a DMAX-3A Rigaku powder diffractometer (Rigaku, Japan). X-ray experiments on crosslinked samples were performed at room temperature. The balance torque of LLDPE/TSCPFLCP composite melt was determined by Haake torque XSS-300 rheometer (Thermo, Germany) at a rotation speed from 10 to 50 rpm. The test temperature was set at 160, 165, 170, 175, and 180 °C, respectively. The rheological properties were measured by a high-pressure capillary rheometer (Rheologic 5000, Ceast, Italy) with a length-to-diameter ratio of 30/1. The tests were performed in a shear rate ranging from 10 to 1500 s^{-1} at 160, 165, 170, 175, and 180 °C, respectively. Morphology and structure of LLDPE/TSCPFLCP blends were observed by scanning electron microscope (SEM, JEOL JSM-5900LV, Japan) and transmission electron microscope (TEM, JEOL JEM-1011, Japan). The samples were fractured in liquid nitrogen, and the fracture surfaces were coated with gold to prevent charging on the surface. Tensile properties of LLDPE/TSCPFLCP blends were measured by an Instron 5967 model materials testing system (USA) according to ASTM D-638 standard. Samples of tension test were dumbbell-shaped and the direction of the tensile force was parallel to the length of samples.

2.3 Synthesis of TSCPFLCPs

M_1, M_2 and PMHS were dissolved in toluene (50 mL) according to the specific feeding proportion as shown in Table 1, then 2.5 mL of $H_2PtCl_6 \cdot 6H_2O$/isopropyl alcohol (0.5 g of hexachloroplatinic acid hydrate dissolved in 100 mL of isopropyl alcohol) was slowly added into the above solution. The reaction proceeded for 72 h at 75 °C under nitrogen and was monitored by FT-IR until the disappearance of the sharp vibrational band at 2166 cm^{-1} assigned as the Si–H stretching. The reaction was ceased by precipitating the mixture into methanol to obtain the crude product, which was further purified by repeated precipitation from methanol after dissolving in chloroform. Finally, white powdery polymers (P1–P6) were obtained and the synthesis route were shown in Fig. 1.

2.4 Preparation of LLDPE/TSCPFLCP blends

LLDPE was dried in a vacuum oven at 80 °C for 12 h prior to processing. The pre-mixed blend of LLDPE and TSCPFLCPs was conducted using a mixer (HAAKE, RS600, Germany) at a temperature of 170 °C and screw speed of 50 rpm for 5 min. After being pulverized and dried, the well-mixed composite was injection-molded into tensile testing bars using a mini-injection system (Thermo Scientific, USA) at melt temperature of 170 °C and the mold temperature of 30 °C. The compositions and code names of the samples were shown in Table 2.

3. Results and discussion

3.1 Characterization of TSCPFLCP

Fig. 2a shows the FT-IR spectra of M_1, M_2 and the representative TSCPFLCP sample P6. It can be seen that the typical peak at 2166 cm^{-1} assignable to the Si–H peak of PMHS disappeared in P6, and the characteristic peak at 1640 cm^{-1} corresponding to the vinyl group of monomers also vanished. In addition, the newly formed Si–O–Si bond showed strong and wide bands between 1000 to 1120 cm^{-1}. All these results indicate that the hydrosilylation reaction between PMHS and monomers proceeded successfully.[23]

Fig. 2b shows ^{1}H-NMR spectra of M_1, M_2 and P6. No vinyl signals of the two monomers at 4.97 and 5.80 ppm were found

Table 1 The polymerization of TSCPFLCP series

Sample	PMHS (mmol)	M_1 (mmol)	M_2 (mmol)
P1	0.25	0.25	1.50
P2	0.25	0.50	1.25
P3	0.25	0.75	1.00
P4	0.25	1.00	0.75
P5	0.25	1.25	0.50
P6	0.25	1.50	0.25

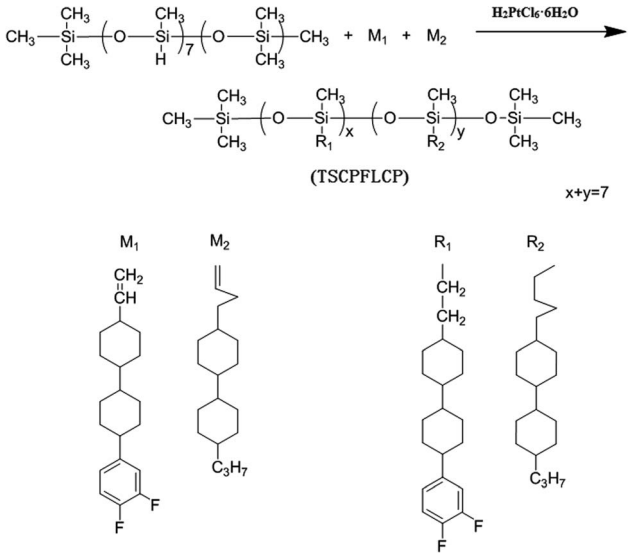

Fig. 1 Synthesis route of TSCPFLCP.

Table 2 Compositions and code names of the sample

Sample	LLDPE (g)	P6 (g)
LLDPE	100	—
LLDPE/P6-0.02%	100	0.02
LLDPE/P6-0.05%	100	0.05
LLDPE/P6-0.1%	100	0.1
LLDPE/P6-0.5%	100	0.5

in the ^{1}H-NMR spectrum of P6, which indicated that the excess monomers were completely removed and P6 was successfully obtained.[24] Based on the integral of typical peaks, the grafted ratio of two monomers in P6 also agreed with the feed ratio.

DSC experiment is used to examine the phase transition of synthesized TSCPFLCPs. Their heating curves the related data are compiled in Fig. 3 and Table 3, respectively. It can be seen

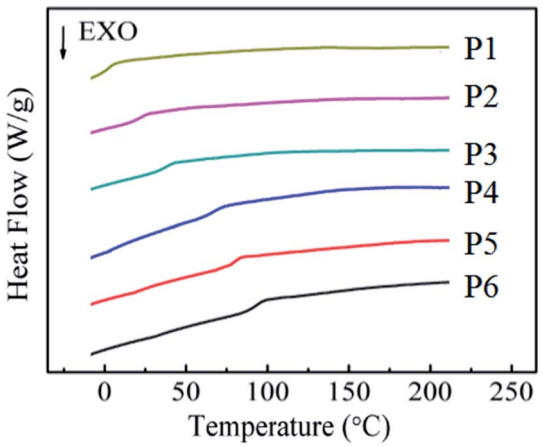

Fig. 3 DSC curves of TSCPFLCP series.

Table 3 Thermal analysis of TSCPFLCP series

	Thermal analysis			
Polymer	T_g (°C)	T_i (°C)	ΔT (°C)	T_d (°C)
P1	−2.7	117.2	120.0	291.4
P2	15.7	140.8	125.2	315.5
P3	35.8	153.3	117.5	330.1
P4	65.4	173.1	107.7	340.0
P5	76.5	180.4	103.8	346.3
P6	86.9	182.4	95.6	335.6

from Fig. 3 that all TSCPFLCPs have obvious glass transition temperature (T_g), indicating they are amorphous liquid crystal polymers. It should be mentioned that no obvious clearing point was detected for the TSCPFLCPs series, which was likely attributed to the small enthalpy change during the liquid crystalline phase transition. With the increase of the content of fluorinated liquid crystal monomer M_1, the T_g and the clearing temperature (T_i) of the polymer increase. The T_g of side chain

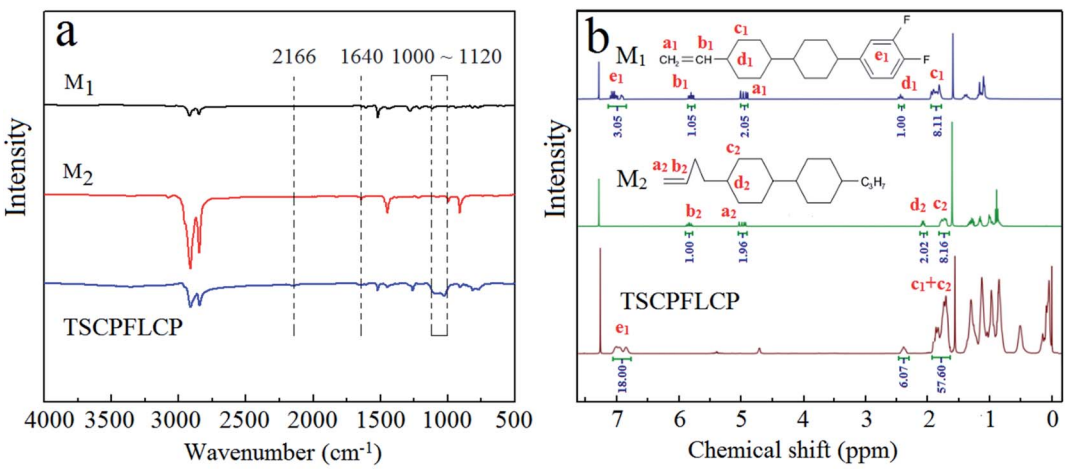

Fig. 2 (a) FT-IR spectra of M_1, M_2 and TSCPFLCP, (b) ^{1}H-NMR spectra of M_1, M_2 and TSCPFLCP in $CDCl_3$.

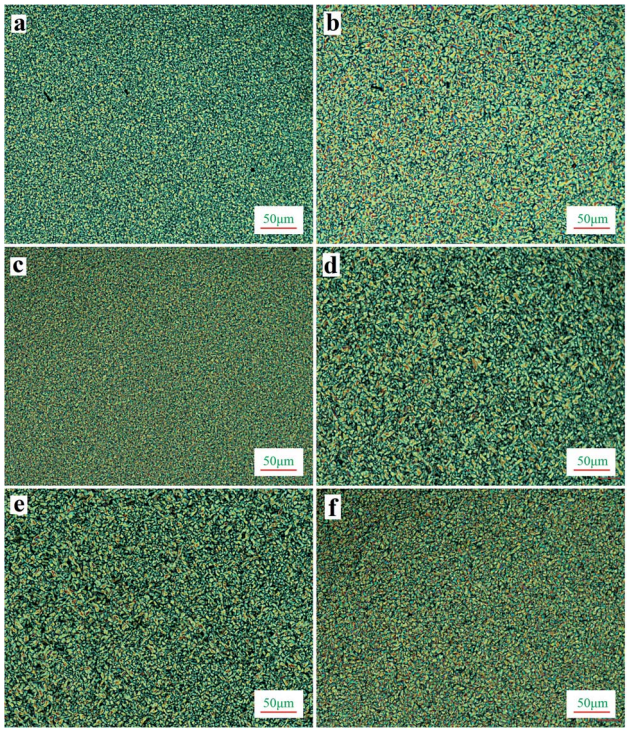

Fig. 4 The texture images of TSCPFLCP series observed by POM:(a) P1 on heating to 100 °C, (b) P2 on heating to 110 °C, (c) P3 on heating to 120 °C, (d) P4 on heating to 140 °C, (e) P5 on heating to 150 °C, (f) P6 on heating to 160 °C.

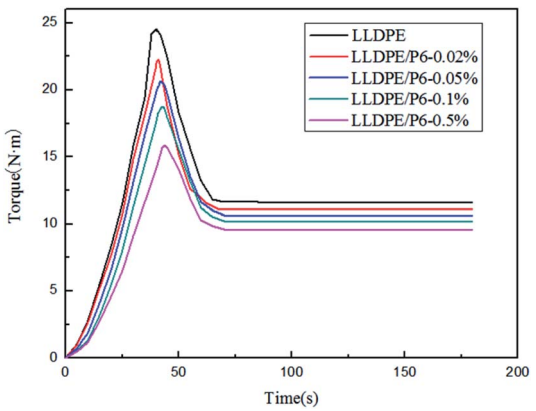

Fig. 5 Torque *versus* time of LLDPE/TSCPFLCP blends with various TSCPFLCP loading.

liquid crystal polymers is closely related to the type of main chain, the rigidity and polarity of liquid crystal units, the volume of side chain groups and the length of flexible spacer connected to the main chain. As for these TSCPFLCPs, although their main chain type and pending flexible spacer have not changed greatly, the increase of rigid and polar M_1 content still makes the movement of molecular segments difficult and leads to the gradual increase of T_g. On the other hand, the rigidity and polarity of fluorine-containing groups restrict their internal rotation, so that the polymers need more enthalpic compensation at higher temperature to drive the intermolecular orientation.

POM equipped with a hot stage is used to observe the liquid–crystalline transition and optical textures. Fig. 4 shows the POM images of TSCPFLCPs at different temperatures. Liquid crystal texture appeared during heating and cooling, indicating that TSCPFLCPs belong to thermotropic double variant liquid crystals. After increasing the temperature above the T_g, the polymer softened and color liquid crystal texture appeared, featuring the broken Schlieren texture of smectic phase. When heated to near the clear point, the crystalline texture disappeared gradually and the field of vision darkened.

Wide angle X-ray diffraction (WAXD) analysis was also performed to verify the crystalline structure. Fig. S1† displays the X-ray diffraction patterns of P6, and the two broad peaks at small angle ($2\theta \approx 5.2°$) and wide angle ($2\theta \approx 20.3°$) are characteristics of smectic phase.[25]

Fig. S2† shows the thermal decomposition process of TSCPFLCPs under nitrogen atmosphere. It revealed that T_d (decomposition temperature at 5 wt% mass loss) are above 290 °C, respectively, indicating their high thermal stability.

Among all the TSCPFLCPs, the thermal properties of P6 (T_g = 86.9 °C, T_i = 182.4 °C, T_d = 335.6 °C) perfectly meet the requirements of processing LLDPE composites (160 ~ 250 °C), and therefore is selected for subsequent blending and extrusion with LLDPE.

3.2 Processability of LLDPE/TSCPFLCP blends

3.2.1 shear rheological properties of LLDPE/TSCPFLCP blends. Torque rheometer is an important instrument to evaluate the processability of polymer materials. Fig. 5 shows the evolution curves of melt torque values of LLDPE/P6 blends at 170 °C and the rotation speed of 50 rpm. The balance torque of the LLDPE/P6 blends diminished gradually with the increase of P6 content. Compared with pure LLDPE (11.85 N m), the balance torque of LLDPE/P6 blend decreased by 6.2%, 9.8%, 13.8% and 19.4% when the P6 contents in the samples were set as 0.02, 0.05, 0.1 and 0.5 wt%, respectively. These results demonstrate clearly that P6 is effective in reducing the melt viscosity. Such an improved processability is likely attributed to the directional orientation of liquid crystalline of P6 into microfibers along the shear direction,[26] which serves as a lubricant to reduce the entanglement between LLDPE molecular chains.[27]

In order to study the influence of the external conditions, such as stress and temperature on the availability of TSCPFLCPs, samples P6-0.5% and LLDPE were selected as the research objects, and the melt torques at different temperatures and speeds were compared. The relationship between the balance torque and rotational speed of the blends at 170 °C is shown in Fig. 6a. It can be seen that the balance torque of LLDPE/P6-0.5% is lower than that of LLDPE, and their torque difference gradually increases with the increase of rotating speed. This result suggests that the molecular orientation of P6 conforms to the shear direction when there is sufficient shear force in the melt processing process. It therefore means that

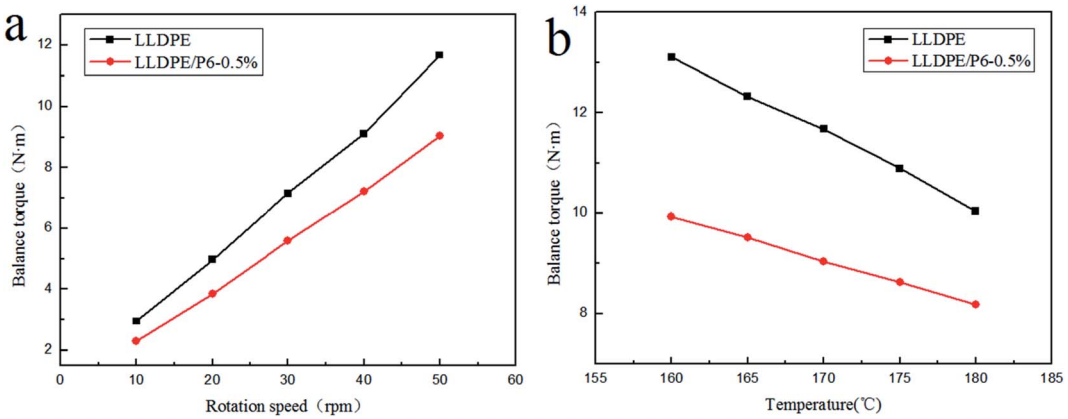

Fig. 6 (a) Balance torque *versus* rotation speed, (b) balance torque *versus* processing temperature.

greater shear force will benefit TSCPFLCP orientation and composite processability.[15,16] Fig. 6b shows the balance torque *versus* temperature curves for LLDPE and LLDPE/P6-0.5% at 50 rpm. With the rising of temperature, the balance torque of both LLDPE and LLDPE/P6-0.5% decreases significantly. Meanwhile, the balance torque of LLDPE/P6-0.5% is significantly lower than that of LLDPE at the same temperature, indicating that the superior processability of LLDPE/P6-0.5% within the whole processing temperature range. When the temperature increased from 160 °C to 180 °C, the balance torque of LLDPE and LLDPE/P6-0.5% decreased by 32.7% and 18.7% respectively. The results show that the addition of P6 reduces the sensitivity of LLDPE to processing temperature. The above results suggest that the processability of LLDPE/TSCPFLCP blends is affected not only by the TSCPFLCP content, but also by the rotational speed (shear force) and processing temperature, which are associated with the orientation of TSCPFLCP during processing.[28]

Fig. 7 shows the relationship between apparent viscosity and shear rate of LLDPE/TSCPFLCP blends and the relationship between shear stress and shear rate at 170 °C. It can be seen that within the experimental range of shear rate, the apparent viscosity and shear stress of the blends gradually decrease with the increase of TSCPFLCP content, which further proves that the addition of TSCPFLCP significantly improves the processability of LLDPE/TSCPFLCP blends.[29]

Fig. 7 shows that the logarithm of shear stress is in linear relationship with the logarithm of shear rate, indicating that the melt flow behavior with TSCPFLCP follows the power-law equation under experimental conditions.[29] According to the power-law equation ($t = K\gamma n$), the power law exponent (n) of LLDPE/TSCPFLCP blends under different TSCPFLCP loads was calculated. As shown in Fig. S3,† the n values of LLDPE/TSCPFLCP blends are less than 1, indicating that the melt of LLDPE/TSCPFLCP blends is a pseudoplastic fluid. When the content of TSCPFLCP increased from 0% to 0.5%, the n value of LLDPE/TSCPFLCP blends increased from 0.33 to 0.45. The results showed that the non-Newtonian properties of LLDPE/TSCPFLCP blends decreased with the increase of TSCPFLCP load. On the basis of the above results, LLDPE/TSCPFLCP blends showed the following features with the increase of TSCPFLCP loads: (1) its non-Newtonian properties decreased; (2) the sensitivity of apparent melt viscosity to shear rate decreases and the processing window widens.

3.2.2 flow activation energy of LLDPE/TSCPFLCP blends. To further investigate the fluidity of composite melt, we

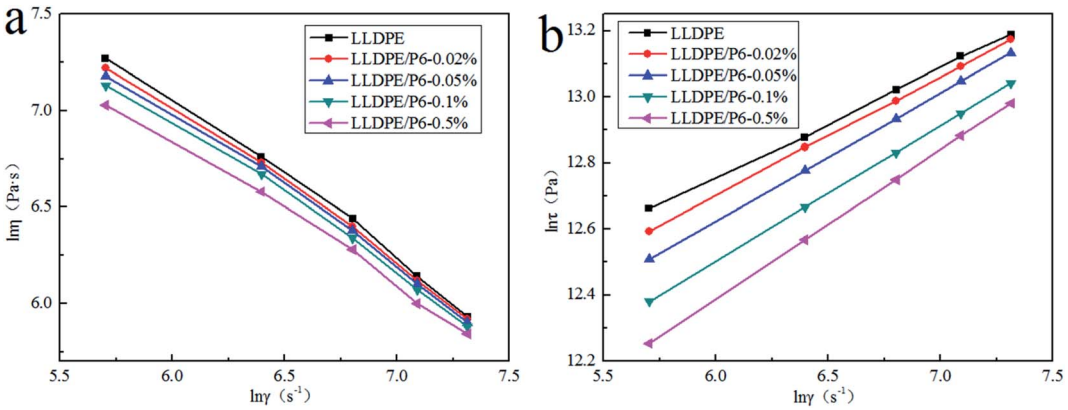

Fig. 7 (a) Apparent viscosity *versus* shear rate at 170 °C, (b) shear stress *versus* shear rate at 170 °C.

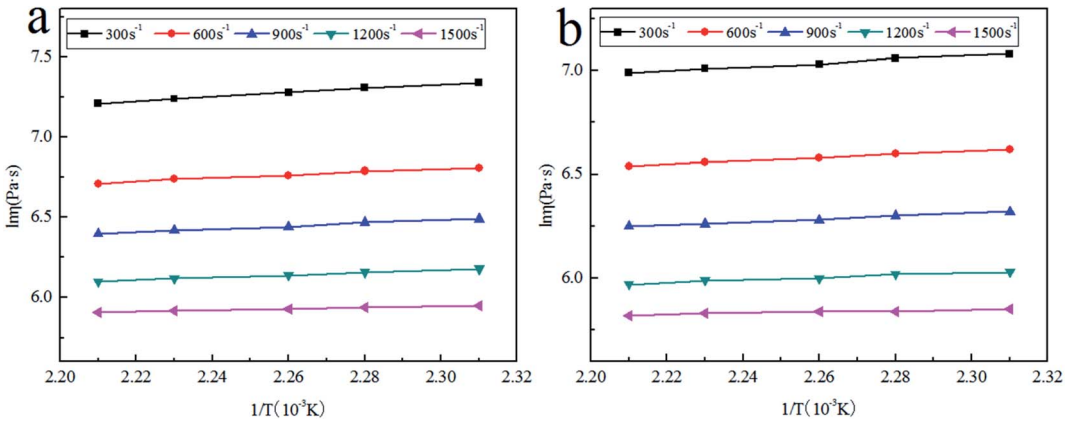

Fig. 8 The logarithm of apparent viscosity (ln η) *versus* 1/T (a) pure LLDPE, (b) LLDPE/P6-0.5% at different shear rates.

Table 4 Values of E_a and R_0 of LLDPE and LLDPE/P6-0.5% at different shear rates

$\gamma(s^{-1})$	300	600	900	1200	1500
$E_{a\ LLDPE}$ (kJ mol^{-1})	10.94	8.23	7.60	6.62	3.31
$E_{a\ LLDPE/P6\text{-}0.5\%}$ (kJ mol^{-1})	7.51	6.53	5.88	4.89	2.28
$R_{0\ LLDPE}$	0.9974	0.9905	0.9931	0.9976	0.9976
$R_{0\ LLDPE/P6\text{-}0.5\%}$	0.9975	0.9975	0.995	0.9926	0.9691

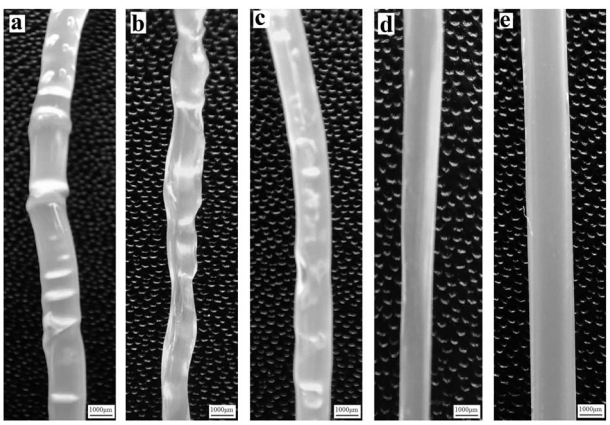

Fig. 9 Optical microscope images of (a) pure LLDPE, (b) LLDPE/P6-0.02%, (c) LLDPE/P6-0.05%, (d) LLDPE/P6-0.1%, (e) LLDPE/P6-0.5%.

calculate the flow activation energy (E_a) by Arrhenius equation $\eta = A \exp(E_a/RT)$. Through logarithmic calculation of Arrhenius equation, we can get the following equation:

$$\ln \eta = \ln A + (E_a/R)(1/T)$$

We plotted the logarithm of apparent viscosity ln η and the reciprocal of temperature at different rotational speeds, and calculate the activation energy from the slope of the curve. Fig. 8 show the relationship between ln η and 1/T for LLDPE and LLDPE/P6-0.5%, respectively. Ln η is increased with 1/T, indicating that the viscosity of the composite melt is gradually decreased with the increase of the processing temperature. It is reasonable because the mobility of the molecular chains is increased under higher temperature, which suppresses the interaction force between molecular chains and thereby reduces the composite viscosity to improve fluidity.[30]

The linear curve of LLDPE at the shear rate of 300 s^{-1} is expressed by the following equation:

$$\ln \eta = 4.31 + 1315.3(1/T)$$

E_a was determined to be 59.4 kJ mol^{-1} from the curve slop. We further calculated the flow activation energy and the linear correlation coefficient (R_0) of other samples, which were listed in Table 4. It is found that the E_a value of LLDPE/P6-0.5% is lower than that of LLDPE at the same shear rate, indicating that LLDPE/P6-0.5% melt is easier to flow, which means 0.5wt% TSCPFLCP could obviously improve the processability of LLDPE. On the other hand, the E_a values of both LLDPE and LLDPE/P6-0.5% are continuously decreased with the increase of shear rate, which is attributed to the disentanglement between molecular chains at high shear rate.[31,32]

3.2.3 Extrusion properties of LLDPE/TSCPFLCP blends. The surface roughness of the blends after extrusion was also observed by optical microscope, and the effect of TSCPFLCP on the melt fracture of LLDPE was investigated. Fig. 9 shows the roughness of LLDPE/TSCPFLCP with different contents. It is obvious that with the increase of TSCPFLCP content, the extrudates of the blends become smoother, showing that TSCPFLCP significantly improves the melt fracture of extrusion. This may be due to the increase of fluorine content improves the polarity of TSCPFLCP, which makes it easier for blend to migrate to the inner wall of the extruder pipe through the melt and coat it on the inner wall of the pipe, serving as an external lubrication.[33,34]

3.3 Mechanical properties of TSCPFLCP blends

As the content of TSCPFLCP increased to 0.5 wt%, the tensile strength increased from 11.4 MPa to 12.6 MPa as shown in Fig. 10a; the elastic modulus of LLDPE containing 0.5%

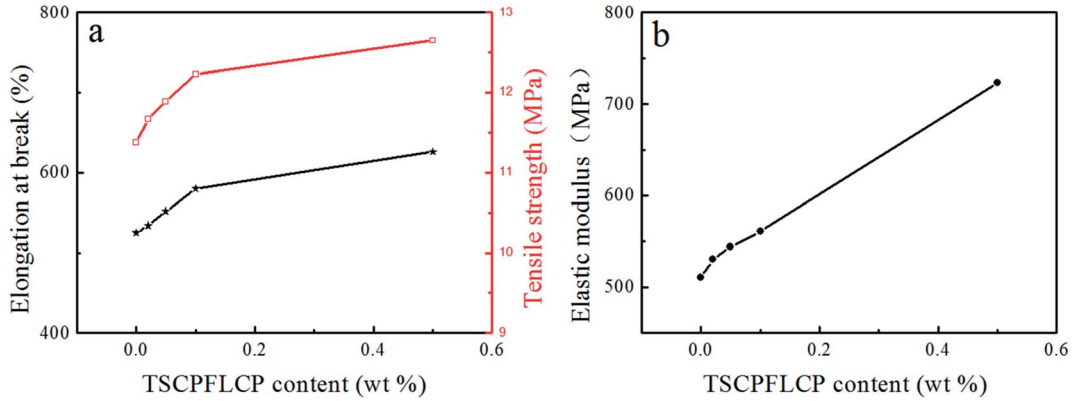

Fig. 10 Effect of TSCPFLCP content on the mechanical properties of blends, (a) elongation at break and tensile modulus, (b) elastic modulus.

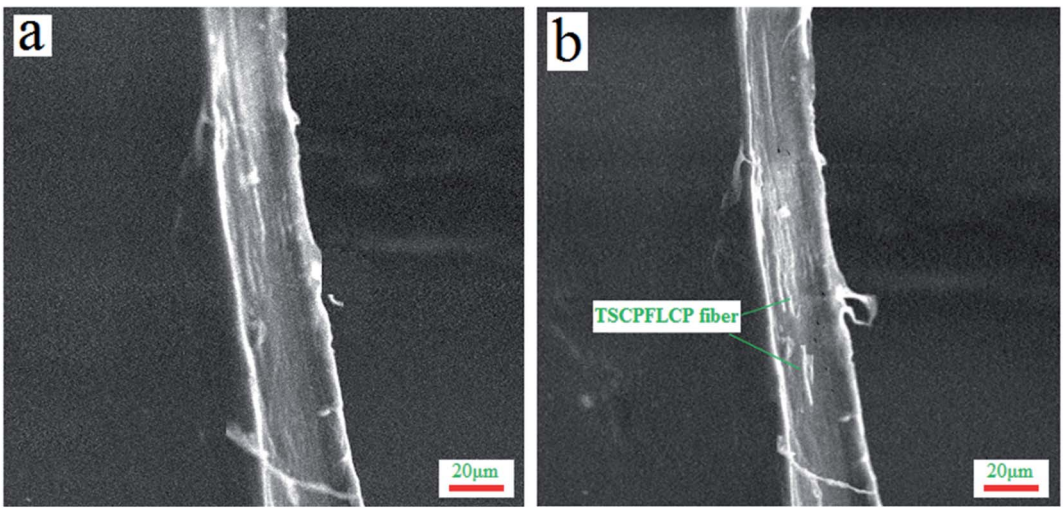

Fig. 11 SEM images obtained from the fracture surface of (a) pure LLDPE, (b) LLDPE/P6-0.5%.

TSCPFLCP was 723.1 MPa, which was significantly increased by 41.6% compare with pure LLDPE. This is because the rigid elements contained in the TSCPFLCP side groups reinforce the composite materials. From Fig. 10b, the elongation at break of LLDPE/TSCPFLCP blends increased from 525% to 626% respectively. This is probably due to the polysiloxane structure in the TSCPFLCP macromolecular chain, as similar toughness strengthening has been observed in composites added with polydimethylsiloxane.[35]

3.4 The facture morphology of LLDPE/TSCPFLCP blends

The influence of TSCPFLCP on the cross-sectional morphology of LLDPE/TSCPFLCP blends was studied by scanning electron microscope and transmission electron microscope. The results are shown in Fig. 11 and S4.† LLDPE was the continuous phase and TSCPFLCP was the dispersed phase. TSCPFLCP forms liquid crystal fibers in the matrix, which explains the improvement of mechanical properties of the blends after adding TSCPFLCP. Because of the poor compatibility between TSCPFLCP and LLDPE, liquid crystal fibers were pulled out of LLDPE matrix, generating noticeable holes on the fracture surface. In addition, more pores were observed in samples with higher TSCPFLCP content, indicating that the formation of more liquid crystal fibers is beneficial for blends processability.

4. Conclusions

A series of polysiloxanes grafted by thermotropic fluorinated mesogenic unit (TSCPFLCP) were newly synthesized to blend with LLDPE for the purpose of improving its processability. Specifically, (1) the balance melt torque of LLDPE (11.85 N·m) decreases by 19.4% when only 0.5 wt% TSCPFLCP is employed in the LLDPE/TSCPFLCP blend; (2) the melt fracture of extrusion was also ameliorated obviously after amending polar fluorine moiety in TSCPFLCP; (3) the introduction of TSCPFLCP weakens the non-Newtonian properties of LLDPE and reduces the flow activation energy, widening the processing window and improves the processing performance. Moreover, the elongation at break of LLDPE increased significantly because of the flexible main chain of TSCPFLCP, accompanied with improvements on tensile strength and elastic modulus. Overall, the

TSCPFLCPs have been demonstrated highly effective in improving the processability of LLDPE, offering an ideal processing aid to enhance its production efficiency.

Conflicts of interest

There are no conflicts to declare.

Notes and references

1 A. Cardelli, G. Ruggeri, M. Calderisi, O. Lednev, C. Cardelli and E. Tombari, *Polym. Degrad. Stab.*, 2012, **97**, 2536–2544.
2 W. Zhou and J. Osby, *Polymer*, 2010, **51**, 1990–1999.
3 T. J. Zolper, A. Seyam, Z. Li, C. Chen, M. Jungk, A. Stammer, T. J. Marks, Y. W. Chung and Q. Wang, *Tribol. Lett.*, 2013, **51**, 365–376.
4 Z. Kokuti, K. V. Gruijthuijsen, M. Jenei, G. T. Molnar and G. Szabo, *Appl. Rheol.*, 2014, **24**, 63984.
5 H. g. He, L. Gao, X. J. Yang, W. Guo, H. Li, T. Xie, S. K. Yang, J. P. Wang, Y. Zhang and X. Y. Yang, *J. Fluorine Chem.*, 2013, **156**, 158–163.
6 H. K. F. Cheng, T. Basu, N. G. Sahoo, L. Li and S. H. Chan, *Polymers*, 2012, **4**, 889–912.
7 L. Zeng, R. Li, P. Chen, J. Xu and P. Liu, *J. Appl. Polym. Sci.*, 2016, **133**, 43800.
8 P. Wei, H. Lou, W. Wang, S. Geng and M. Jiao, *Liq. Cryst.*, 2021, **48**, 466–474.
9 K. Oh, H. Kim and Y. Seo, *RSC Adv.*, 2019, **9**, 12189–12194.
10 C. Y. Ren and P. Gao, *Polymer*, 2012, **53**, 3958–3967.
11 L. C. Wu, P. Chen, J. Chen, J. Zhang and J. S. He, *Polym. Eng. Sci.*, 2007, **47**, 757–764.
12 A. B. Samui, S. Pandey and S. P. Mishra, *RSC Adv.*, 2015, **5**, 68351.
13 F. Chen, Y. Cong and B. Zhang, *Liq. Cryst.*, 2016, **43**, 1100.
14 X. Guan, B. Cao, J. Cai, Z. Ye, X. Lu, H. Huang, S. Liu and J. Zhao, *Polymers*, 2020, **12**, 911.
15 A. K. Kalkar, V. D. Deshpande and M. J. Kulkarni, *J. Polym. Sci., Polym. Phys.*, 2010, **48**, 1070–1100.
16 Y. Rong, L. Chen, W. Q. Zhang, H. B. Chen and Y. Z. Wang, *Polymer*, 2011, **52**, 4150–4157.
17 Y. Xia, H. Zhang, Q. Wang, J. Guo and Y. Gong, *J. Thermoplast. Compos. Mater.*, 2016, **29**, 37–47.
18 D. R. Arda and M. R. Mackley, *J. Non-Newtonian Fluid Mech.*, 2005, **126**, 47–61.
19 C. W. Stewart, *J. Rheol.*, 1993, **37**, 499–513.
20 M. A. Apfel, H. Finkelmann, G. M. Janini, R. J. Laub, B. H. Luehmann, A. Price, W. L. Roberts, T. J. Shaw and C. A. Smith, *Anal. Chem.*, 1985, **57**, 651–658.
21 Y. Jin, R. Fu, Z. Guan, J. Gong and B. Li, *J. Chromatogr. A*, 1989, **483**, 394–400.
22 H. Finkelmann, H. J. Kock and G. Rehage, *Makromol. Chem., Rapid Commun.*, 1981, **2**, 317–322.
23 J. S. Hu, B. Y. Zhang, A. J. Zhou, L. Q. Yang and W. Bai, *Eur. Polym. J.*, 2006, **42**, 2849–2858.
24 W. Yao, Y. Gao, C. Zhang, C. Li, F. Li, Z. Yang and L. Zhang, *J. Polym. Sci., Polym. Chem.*, 2017, **55**, 1765–1772.
25 W. Wu, Z. Li and B. Zhang, *Liq. Cryst.*, 2021, **48**, 1723–1732.
26 T. M. Malik, P. J. Carreau and N. Chapleau, *Polym. Eng. Sci.*, 1989, **29**, 600–608.
27 J. H. Chang, B. K. Choi, J. H. Kim, S. M. Lee and M. S. Bang, *Polym. Eng. Sci.*, 2010, **37**, 1564–1571.
28 S. C. Hong, L. Yang and F. Gao, *Compos. Sci. Technol.*, 2002, **62**, 757–765.
29 M. Nanda and D. K. Tripathy, *J. Appl. Polym. Sci.*, 2012, **126**, 46–55.
30 S. Thalib, S. Huzni, S. Fonna, C. H. Azhari and S. Zakaria, *IOP Conf. Ser.: Mater. Sci. Eng.*, 2019, **602**, 012086.
31 N. Muksing, M. Nithitanakul, B. P. Grady and R. Magaraphan, *Polym. Test.*, 2008, **27**, 470–479.
32 M. Hemmati, G. H. Rahimi, A. B. Kaganj, S. Sepehri and A. M. Rashidi, *J. Macromol. Sci. B.*, 2008, **47**, 1176–1187.
33 F. N. Cogswell, *J. Non-Newtonian Fluid Mech.*, 1977, **2**, 37–47.
34 S. G. Hatzikiriakos, *Polym. Eng. Sci.*, 1994, **34**, 1441–1449.
35 X. Chen, J. Yu and S. Guo, *J. Appl. Polym. Sci.*, 2006, **102**, 4943–4951.